Benajes Calvo, JV.; López Sánchez, JJ.; Molina Alcaide, SA.; Redón Lurbe, P. (2015). New 0-D methodology for predicting NO formation under continuously varying temperature and mixture composition conditions. Energy Conversion and Management. 91:367-376. doi:10.1016/j.enconman.2014.12.010.

New 0-D Methodology for Predicting NO Formation under continuously varying temperature and mixture composition conditions

J. Benajes, J. J. López, S. Molina, P. Redón[1]

CMT-Motores Térmicos, Universitat Politècnica de València

[1] Corresponding author: Pau Redon. CMT-Motores Termicos, Universitat Politècnica de València. C/ Camino de Vera s/n, Postal Code: 46022, Valencia, Spain. Phone: +34 961405302, email: paredlur@gmail.com.

New 0-D Methodology for Predicting NO Formation under continuously varying temperature and mixture composition conditions

J. Benajes, J. J. López, S. Molina, P. Redón

CMT-Motores Térmicos, Universitat Politècnica de València

0. Abstract

The development of new diesel combustion modes characterized by low combustion temperatures, to minimize the NO_x emissions, has caused a noticeable change in the diesel spray's structure and in the NO_x chemistry, gaining relevance the N_2O and the prompt routes in detriment of the thermal mechanism. Therefore, to accurately predict the NO_x emissions, the detailed chemistry and physics must be taken into account, with the consequence of increasing the computational cost.

The authors propose in the current study a new predictive methodology associated to low computational cost, where detailed chemistry and simplified physics are considered. To diminish even more the computational cost, the chemistry was tabulated as a function of temperature and oxygen excess mass fraction (parameter which effectively couples the equivalence ratio and the EGR rate). This tool has been developed with the objective of being applicable in continuously varying temperature and mixture fraction conditions (the diffusion diesel spray context) and was validated with the Two-Stage Lagrangian model (TSL-model) and with real engine measurements.

The results in both validation scenarios reflect a high degree of accuracy making it applicable, at least, to perform qualitative predictions. By extension, it is expected to perform similarly in continuously varying temperature conditions (i.e: homogenous charge compression ignition diesel combustion modes) which are less demanding computationally speaking.

1. Introduction

The development of new diesel combustion modes characterized by low combustion temperatures, to minimize the NO_x emissions, has caused to diminish the relevancy of the thermal mechanism with respect to the total NO_x formation. This fact was analyzed by Desantes et al. [1] for conventional diesel combustion (CDC) and low temperature combustion (LTC) conditions. In this work, where LTC conditions were defined assuming a similar criteria to the one used by Musculus [2] (i.e. adiabatic combustion temperature lower than 2200K), the authors corroborated that the thermal mechanism reduces its relevancy to a 40%-60% independently of the fuel (n-heptane or methane) and the equivalence ratio considered ($0.5 < \Phi < 1$).

Focusing on this latter aspect, the combustion of leaner fuel-oxidizer mixtures not only reduces the thermal mechanism [3] influence by decreasing the combustion temperature but also modifies the chemistry of the NO formation process and therefore other pathways like the N_2O intermediate [4-6] can become relevant. On the one hand combustion of leaner mixtures are typically employed, in the premixed auto-ignition diesel combustion contexts (e.g: HCCI mode), to achieve low combustion temperatures with little exhaust gas recirculation (EGR) to mitigate the important drawbacks associated with the employment of massive EGR. These conditions cause the N_2O pathway to gain in importance as several authors have already demonstrated [7-8]. On the other hand, in the context of diffusion diesel sprays, Musculus [2] observed that the NO_x were formed inside the fuel spray where the variation of local conditions reflect a leaner mixture ($0.5 < \Phi < 1.5$) in comparison with CDC conditions summarized in Dec's model [9]. This fact not only corroborates how the N_2O route gains relevancy, just as in the previous context, but also highlights the need of taking into account the prompt mechanism [4, 6, 10-11] which becomes relevant in fuel rich mixtures ($\Phi > 1$).

Independently of the combustion scenario under analysis, it seems clear the need to consider not only the physical phenomena behind these combustion processes but also all the pathways involved in the NO_x chemistry in order to accurately predict the emissions of this pollutant.

This asseveration is undoubtedly associated with a substantial increase of the computational costs of the corresponding simulations. Some authors have focused, from long time ago, on reducing it by analyzing the physical phenomena in detriment of simplifying the chemistry of the combustion process. To do so, new computational tools have been created based on: partial-equilibrium assumptions [12-13], constrain equilibrium [14-16], computational singular perturbation [17] and tabulated chemistry. Multiple procedures have been developed relaying on this latter concept. Initially, Pope [18] developed the in-situ adaptive tabulation methodology (ISAT) which was the first attempt to tabulate the chemistry. It consisted in characterizing the thermochemical state of a mixture, at any time and point, by the mass fraction of a number of species, the enthalpy and the pressure variables. However, this methodology derived to the intake low dimension manifold procedure (ILDM) [19] which simplified the reduction of the chemical schemes and therefore the generation of look-up tables. However its main inconvenience is the low accuracy at low temperatures, where higher manifold is required. To solve this inconvenience, the flame propagation of ILDM approach (FPI) [20-21] was developed as well as the flamelet generated manifold (FGM) [22-23]. Even though these latter ones are used nowadays, the great inconvenience of all these tools is considering assumptions of uncertain generality and accuracy, the tedious task of determining the key species and parameters to describe the mixture thermodynamically, the construction of the tables where the different species' concentrations are summarized and which require huge memory resources, and the degree of knowledge required to understand the fundamentals on which these computational tools are sustained on.

99 Another way to reduce computational cost is to simplify the physics involved in the
100 process and concentrate on the chemistry by employing complete mechanisms, including high
101 number of species and reactions. Commonly, this is achieved mainly by reducing the number
102 of dimensions to be considered, e.g.: 1-D and 0-D models. Regarding the 0-D models, the most
103 extended approaches are related to: single-zone homogeneous in-cylinder conditions [24],
104 two-zone [25] and multi-zone combustion models [26]. As Zheng pointed out in [27], even
105 though the single zone cannot be used to obtain results referred to spatial distribution, they
106 are more efficient in capturing the detailed chemical kinetics and the basic thermodynamic
107 events. Several research studies [27-31] analyzing how the pollutant emissions formation
108 processes are affected by different operating conditions, (pressure, intake temperature,
109 exhaust gas recirculation rate and fuel chemistry) have used such models.

110 Consequently, the authors believe that despite the drawbacks associated with the
111 tabulated chemistry there is undoubtedly a great potential in combining it with the 0-D models
112 to perform fast and accurate pollutant predictions.

113 2.- Objectives and General Methodology

114 2.1- Objectives

115 The objective of this study is to develop a new methodology, based on the coupling of
116 a reduced n-heptane mechanism and a detailed NO_x sub-mechanism, capable to minimize the
117 major drawbacks of employing tabulated chemistry and to accurately predict the NO
118 formation trends under **continuously varying temperature (T) and relative mixture fraction**
119 (Z_r) conditions (like in diesel diffusion flames). Moreover, this tool should be able to run over a
120 wide range of combustion conditions independently of any specialized commercial chemical
121 kinetic software and without the need of advanced modeling knowledge and computational
122 resources.

This particular scenario has been chosen because current commercial diesel engines are still operating under the diffusion diesel spray context and it is more computationally challenging compared with those where exclusively the temperature varies with time (i.e: auto-ignition premixed combustion modes).

2.2.- General methodology

To achieve the established objective a three-stage procedure was followed in which the first of them dealt with the developing of the proposed methodology by using the Chemkin Pro software [32], in particular the closed perfectly stirred reactor 0-D model (cPSR model). The second and third stages consisted in checking the effectiveness of the proposed methodology in diesel sprays simulations and against real engine's measurements by employing the Two-Stage Lagrangian model (TSL) [33] and the apparent combustion time model (ACT) [34], respectively.

This methodology was developed using a chemical kinetic mechanism made up of combining the Seiser et al. n-heptane reduced mechanism [35] with a detailed NO_x sub-mechanism included in the GRI-mech 3.0 [36]. The resulting mechanism will be denoted as RES_{TOTAL}-mechanism and consists of 181 species and 1583 reactions. The use of this widely extended mono-component fuel surrogate, with a similar cetane number as typical European diesel fuel, could discard the NO formation routes associated with the nitrogen and aromatic contents of the fuel and not be the most appropriate for low temperature combustion cases. Regarding the influence of fuel contribution with NO formation, both contributions were found to be negligible in [1, 38-39]. With respect to low temperature combustion processes, several other aspects were considered, like: available kinetic mechanisms of new proposed compounds or blends, their reliability and experimental validation and the computational cost required.

147 Finally, to minimize the drawbacks of tabulated chemistry, this research will focus on
148 the NO formation rates to predict NO_x formation. Considering exclusively NO will not influence
149 significantly the results because as concluded in [40] the role of the combustion process in the
150 NO_2 formation process is minor under current diesel engine conditions.

151 ## 3. Detailed description of the proposed methodology

152 In this section the proposed methodology will be explained in detail, focusing on the
153 theoretical principles and hypothesis considered as well as on how it works.

154 ### 3.1.- Theoretical principles

155 In the following lines a brief review of how some key variables (temperature, relative
156 mixture fraction, time, EGR rate and pressure) influence the NO prediction will be performed
157 focusing on a steady state diesel diffusion flame.

158 - Temperature (T): Parameter which varies, along the axial coordinate, from the
159 fuel's temperature to the combustion's temperature, reached at the flame
160 front region, and then decreases. This is due to a sequence of processes such
161 as: premixed combustion, mixing phenomena with combustion products
162 formed in the flame front region, diffusion combustion and dilution of the
163 combustion products by remaining fresh oxidizer. The temperature reached at
164 the flame front will undoubtedly determine the formation of this pollutant in
165 the region where most NO is expected to be formed.
166 - Relative mixture fraction (Z_r): Variable describing the fuel-air ratio in a
167 particular mixture and key factor to the NO chemistry. It diminishes along the
168 axial coordinate, distinguishing three main regions; fuel-rich ($Z_r > 1$),
169 stoichiometric ($Z_r = 1$) and fuel-lean conditions ($Z_r < 1$). In each of these regions
170 a different NO formation route is predominant.

- Time (t): The time variable strongly influences the NO chemistry as a consequence of the time dependence of the two previous key parameters. Moreover, the initial working conditions themselves influence the time evolution of these parameters.
- Exhaust gas recirculation rate (EGR rate): This variable influences indirectly the NO chemistry by reducing the combustion temperature as a consequence of diluting the oxidizer stream with combustion products which are less reactive. Therefore it determines the initial oxygen mass fraction (Y_{O2ini}) available to react. This last characteristic, the Y_{O2ini}, will be used to define the EGR rate of the different cases presented along the whole research study.
- Pressure (P): This variable has a minor impact on the NO chemistry and it can be considered to remain constant throughout the whole diesel spray. However, since it can be very different depending on the injection timing (due to compression and expansion in the cylinder), it will be included in the model.

From the previous review it is plausible that Z_r and EGR rate are closely related to the oxidizer stream, specially with the oxygen content. Therefore several authors, like Peters [41] and Payri [42], in an attempt to agglutinate both variables in a single one, have come up with a mathematical expression, like the following:

$$Y_{O2exc} = Y_{O2ini} * (1-Z_r) \quad \text{(Eq.1)}$$

where Y_{O2exc} is the oxygen excess mass fraction, Y_{O2ini} quantifies the content of oxygen available initially in the combustion chamber and Zr describes the fuel-air relative mixture fraction.

To confirm that this variable really agglutinates both of them, a parametric study (varying Z_r between 0.2 and 1) was performed for two different EGR rates (Y_{O2ini}: 0.23 and 0.1).

In order to discard the effect of the initial conditions on the temporal evolution of NO, equilibrium state was considered for two given temperatures, 1500K and 2500K. These temperatures were selected to analyze the behavior of Y_{O2exc} under two premises:

- Close to typical combustion temperatures in different combustion modes, like: low temperature combustion (LTC), 1800K ≤ T ≤ 2200K, and conventional diesel combustion (CDC), T > 2200K.
- With the temperature range previously described, the thermal mechanism can mask the "real" behavior of the tested variable due to the strong temperature dependency. Consequently, the 1500K temperature value was chosen to mitigate this effect while respecting the first premise.

The results obtained from the EQUIL module of Chemkin Pro were plotted in Figures 1a and 1b. These illustrate that identical NO_{eq} values are achieved, at a given $Y_{O2exc,}$ for both cases and therefore corroborating that this parameter can be used to relate Z_r and EGR rate (Y_{O2ini}) in a single variable. Therefore Y_{O2exc} is going to be employed throughout the present study because it reduces the number of variables to characterize.

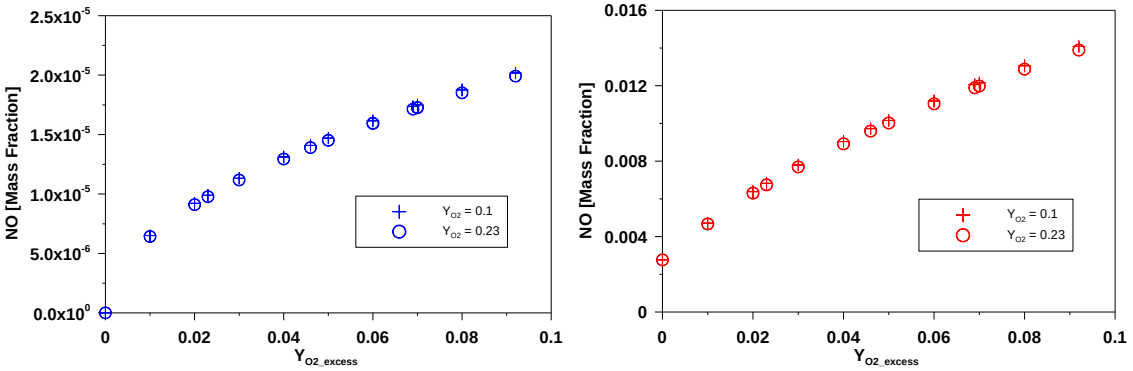

a) **b)**

Figure 1.- Comparison of the NO values for a given oxygen excess mass fraction determined by different relative equivalence ratios and initial oxygen mass fraction (used to characterize the EGR rate), at equilibrium conditions and for two temperatures, a) 1500K and b) 2500K.

3.2.- Description of the hypothesis and the methodology's development procedure

After reviewing the key variables related to the NO formation process, the authors realized that T and Y_{O2exc} where the predominant parameters and to a lesser extent P. Therefore the following hypothesis was considered: **the NO evolution, for any given combustion process, can be determined just considering the temporal evolution of temperature, pressure and Y_{O2exc} variables. This evolution can be reproduced by the concatenation of a finite number of infinitesimally small processes at constant T, Y_{O2exc} and P**.

Consequently, based on the previous hypothesis, the NO formation process has to be studied at constant T, P and YO2exc. For this reason non-steady state simulations using the cPSR model from Chemkin Pro were performed to obtain the temporal evolution of NO (NO(t)) at constant T, Y_{O2exc} and P conditions for different relative mixture fraction values ($0.2 \leq Zr \leq 1$). The considered simulation time was of 1s to guarantee an effective future characterization of all the studied conditions, including the slowest ones. Additionally, in an attempt of minimizing the number of simulations required, only the non-EGR scenario was taken into account. It is easily demonstrable, using equation 1, that by doing so all the other EGR rates are also being indirectly considered.

Afterwards, to make comparable all the studied conditions, a normalization process was encountered in which NO(t) was normalized by the corresponding NO equilibrium composition (NO_{eq}) using the EQUIL module of Chemkin Pro. These equilibrium values were stored in a look-up table as a function of T, Y_{O2exc} and P. Finally the resulting evolution plotted in Figure 2 were accurately characterized by an exponential fit equation, equation 2 (Eq.2).

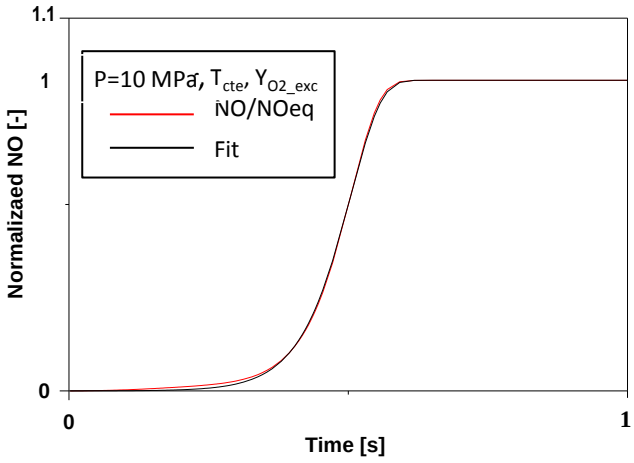

Figure 2.- Temporal evolution of normalized NO and its fit for a given temperature, pressure and oxygen excess mass fraction.

$$\frac{NO}{NO_{eq}} = 1 - \exp(-k * t) \qquad \textit{(Eq. 2)}$$

where NO is the amount of this pollutant predicted at a certain time, NO_{eq} is the amount of NO formed in equilibrium state for the corresponding working conditions, k is a constant value which characterizes the NO/NO_{eq} evolution and t is the elapsed time. The k value will be tabulated in a second look-up table function of T, Y_{O2exc} and P.

The great advantage of this fit mainly relies in three factors:

- This trend highlights the fact that the NO formation chemistry behaves similarly as a single pseudo first order reversible reaction [43] simplifying drastically the chemical mechanisms related with the NO_x formation. This is mathematically demonstrated in Appendix A.
- The whole normalized temporal evolution is described by just one variable, k, which can be stored in a look-up table as a function of T and Y_{O2exc} (Figure Figure 2).

- The equation in its differential form (Eq. 3), employed to concatenate the sequential processes, is simple and requires low computational cost. In Appendix B, the mathematical demonstration of how equation 3 is achieved from its predecesor, equation 2, is summarized.

$$\mathbf{NO_t = NO_{t-1} + k * (NO_{eq} - NO_{t-1}) * (t_t - t_{t-1})} \quad \mathbf{(Eq.3)}$$

where NO_t is the NO calculated at each considered time (t), NO_{t-1} is the calculated amount of NO in the previous time step and k is the empirical exponential fit constant. The NO composition at equilibrium conditions for a given T, P and Z_r is denoted as NO_{eq} and (t_t-t_{t-1}) is the considered time step, which can be constant or variable.

The resulting look-up tables from the described procedure are represented in Figure 3a and 3b for a given pressure (10 MPa). The first plot corresponds to NO_{eq} values calculated under constant pressure and temperature conditions with the purpose of generating a look-up table in which NO_{eq} is a function of YO2excess and T. Looking closely at this plot seems that the results are in contradiction with the fact that for a given initial temperature the NO increases for $0.2 \leq \Phi \leq 0.78$ and then diminishes for $0.78 < \Phi \leq 2$ [44]. However these discrepancies are consequence of the constant temperature constrain. Under these conditions, the NO formation is exclusively dependent on the oxygen content and not in the Φ. This explains why higher NO formation is achieved for leaner fuel mixtures (higher YO2excess) in contrast, with the optimum, 0.78, found in [44]. In this latter scenario, higher Φ leads to a higher combustion temperature but also reduces the oxygen availability.

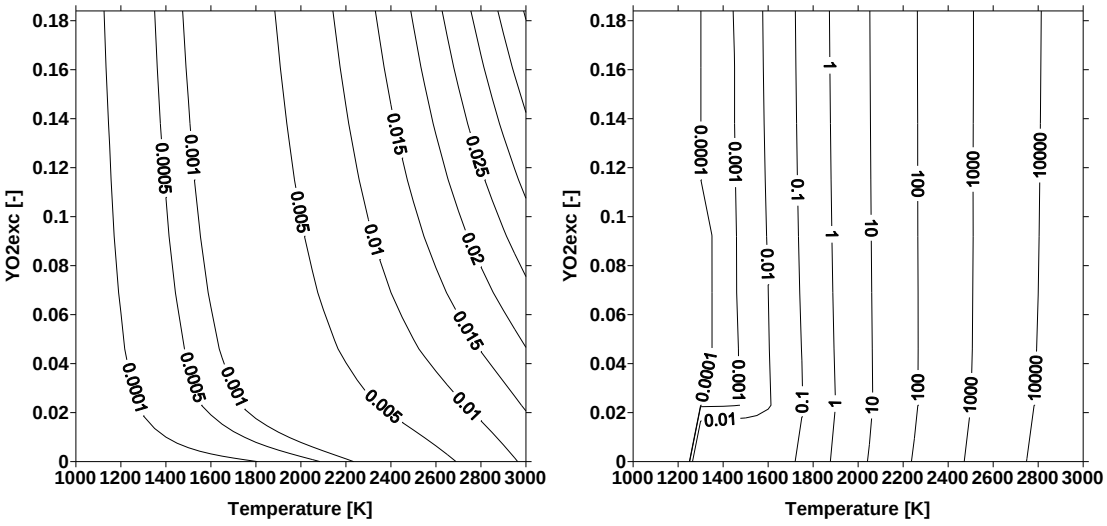

a) *b)*

Figure 3.- Results yield from the constant temperature characterization process of NO formation over the considered operational range for n-heptane as diesel fuel surrogate and at 10MPa; a) NO equilibrium composition, b) the k values characterizing the normalize NO formation rate.

The results summarized in Figure 3b, calculated under constant pressure and enthalpy conditions, are coherent with the chemical kinetic principles (higher temperatures cause an increase in reaction rates leading to higher k values) and with the chemistry ruling the NO formation process. At high temperatures (T > 1800K) the thermal mechanism, strongly dependent on this parameter, is the predominant formation route. This explains the vertical iso-k lines in this region. As the temperature decreases (T < 1800K) so does its contribution in favor of the prompt and the N_2O pathways. This explains the slight curvature of the iso-k lines and the observed distortions for $Y_{O2exc} < 0.05$.

Finally, the predicted NO formation trend will be determine by applying equation 3 which is dependent on these two constants.

3.3.- Implementation of the proposed methodology

With the k and the NO_{eq} tables generated and in coherence with the theoretical principles ruling the NO chemistry, the methodology can be implemented and checked.

Initially, the TSL model [33] was used as a reference tool in a diesel diffusion flame to obtain: T(t), $Y_{O2exc}(t)$ and the NO time-evolution ($NO_{REF}(t)$) for a given initial working condition, described by P, Y_{O2ini} and T, respectively. This model was proposed by Broadwell and Lutz to perform 1-D simulations to calculate temperature and composition (predict NO_x and soot emissions) in stationary, turbulent and non-premixed diesel sprays with a low computational cost by simplifying the flame structure in two regions: flame front and flame core. Each of them is characterized by a perfectly stirred reactor (PSR) which move in parallel, exchanging mass and temperature between them, as they move downstream the stationary spray, see Figure 3. This simplification allows studying of the chemical processes inside the flame structure by considering detailed kinetic mechanisms. In this case, the mechanism used was RES-Mech, the resulting from combining the Seiser et al mechanism [35] with the NOx sub-mechanism of GRI Mech 3.0 [36].

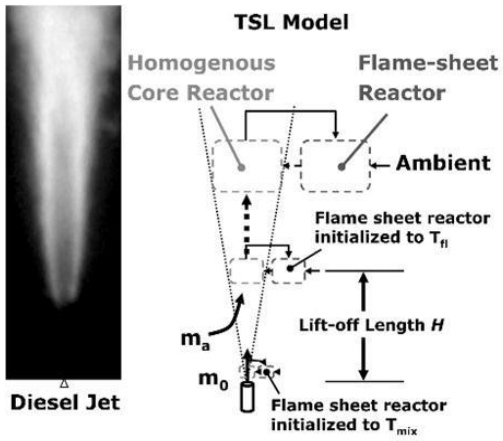

Figure 4.- Schematic representation of the how the two-stage Lagrangian model (TSL model) simplifies the diesel flame in two regions: flame core and flame front [33].

These results will be the input variables to determine the k and the NO_{eq} values from the look-up tables. Substituting these values into equation 3 and knowing the time step, given also by the reference tool, the predicted NO trend (NO_{MET}) is obtained. In this case, the index

319 "MET" stands for proposed methodology, or in other words, the methodology developed in
320 the present paper. To check its accuracy, this trend will be afterwards compared with NO_{REF}.

321 4. Results

322 In this section the predictive capability of the proposed methodology will be presented
323 and analyzed by comparing it with NO_{REF} under continuously varying temperature and relative
324 mixture fraction conditions (e.g: diesel diffusion flame scenario) considering non-EGR and EGR
325 cases. Additionally, validation studies were performed with real engine-out NO_x emissions
326 obtained for a wide range of operational conditions, covering LTC and CDC combustions,
327 running the engine under diffusion diesel combustion characteristics.

328

Parameter	Value
Pressure [MPa]	10
Fuel	n-heptane
Nozzle orifice diameter [μm]	100
Injection velocity [m/s]	630
Fuel density [kg/m^3]	613

329

330 ***Table 1.- Summary of the baseline conditions considered in the TSL model.***

331

Cases	T_{oxi} [K]	T_{fuel} [K]	P [Mpa]	Y_{O2ini} [-]
Case non-EGR	1000	300	10	0.23
Case EGR	1000	300	10	0.1

332

333 ***Table 2.- Summary of the considered conditions for the two studied cases.***

334 4.1.- Continuously varying temperature and relative mixture fraction conditions

335 To check the accuracy of the proposed methodology in this context, the TSL model was
336 used to simulate the behavior of a diesel diffusion flame for two cases non-EGR (Y_{O2ini} = 0.23)
337 and massive EGR rate (Y_{O2ini} = 0.1), summarized in Table 21 using the baseline conditions listed
338 in Table 2 [45]

The temporal evolution of T and Z_r (top row) as well as NO_{REF} (bottom row) are plotted for both cases in Figures 5a and 5b. In these plots, the stoichiometric condition (Z_r = 1), typical of the flame front region, is depicted by a discontinuous line limiting the fuel-rich (left hand side) and the fuel-lean regions (right hand side).

These results agree with the theoretical principles ruling diesel sprays, under CDC [[9] and LTC conditions [2], and the Z_r value was used to calculate the corresponding Y_{O2exc}. It is worthy to highlight that the decrease in the amount of NO in the fuel-lean region is due to dilution effects caused by the mixing of oxidizer with the combustion products as they move downstream from the flame front region.

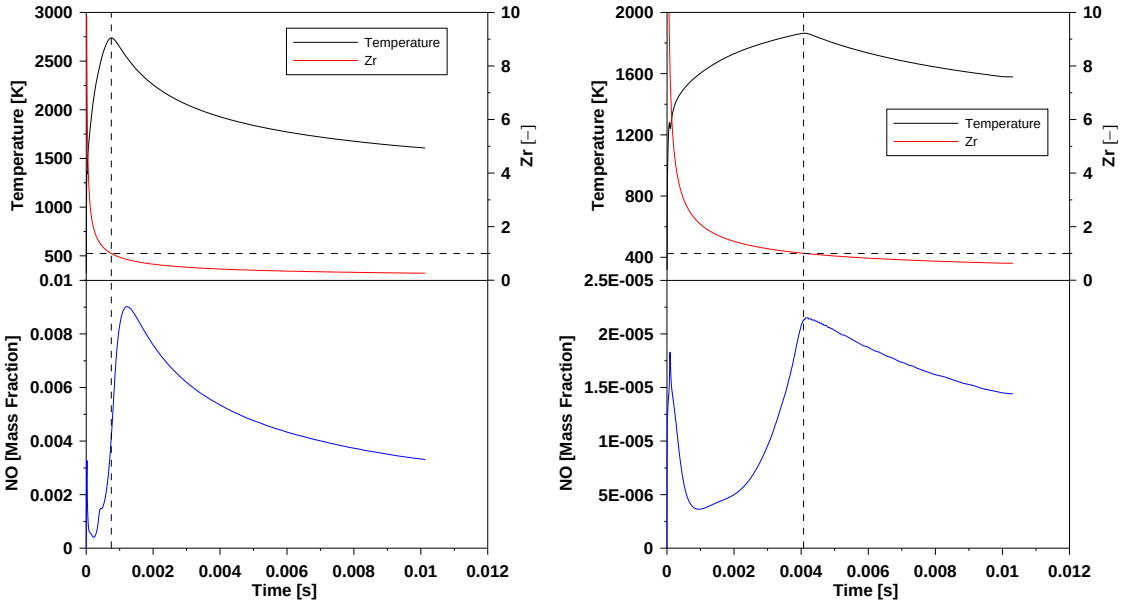

Figure 5.- Temperature, mixture fraction and NO evolution along the axial axis of a diesel diffusion flame simulated by the TSL model with the baseline conditions summarized in Table 11. a) Non-EGR case (Y_{O2ini}=0.23) and b) massive EGR case (Y_{O2ini}=0.1).

Despite the fact that the proposed methodology is built focusing on this latter region, higher amounts of NO are expected to be formed , it was validated considering the whole

evolution of the spray structure in the axial coordinate. In order to take into account the flame front inner region, where $Z_r > 1$, the Y_{O2exc} was considered to be 0 as well as the initial NO.

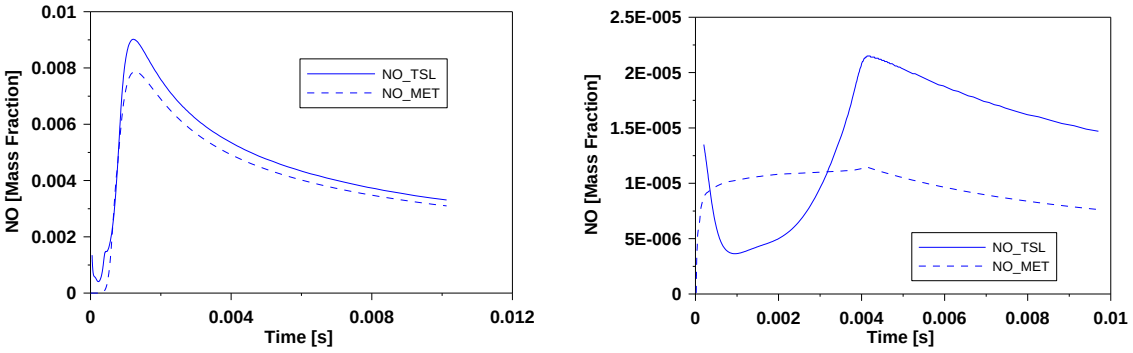

a) **b)**

Figure 6.- Comparison of the NO time evolution between the TSL model and the methodology proposed in this research paper. a) Non-EGR case (Y_{O2ini}=0.23) and b) massive EGR case (Y_{O2ini}=0.1).

Generally speaking Figure 6a and 6b highlight that the proposed methodology has a high accuracy for the case with no EGR in contrast with the one with massive EGR. This can be explained by the strong temperature dependency of the NO formation process. In other words, the exponential fit is less accurate at lower temperatures (massive EGR) than at higher because the process is extremely slow and very little NO is formed. This is corroborated in Figure 6b where there is a lower predictive accuracy than in Figure 6a where higher combustion temperatures are reached.

However, in both cases the accuracy diminishes in the inner region of the flame (left hand-side of the peak value). In the first case, non-EGR, the proposed methodology underestimates while in the second, massive EGR, it overestimates the amount of NO. In this latter case, this is clearly a consequence of not considering the NOx reburning phenomenon, responsible for the NO reduction by converting them into HCN or HCNO in presence of hydrocarbons and low temperatures, 800-1500K [46]. Despite the fact that several more

377 recent studies have corroborated its existence in internal combustion engines [42, 47-48] the
378 authors decided not to include it in this proposed methodology for simplification reasons.

379 In an attempt of achieving higher accuracy, especially for the massive EGR case, the
380 authors hypothesized the existence of other phenomena, distinct to those described
381 previously, strongly involved with the NO formation process in the diesel diffusion flame
382 context rather than a problem associated with the proposed methodology.

383 From the results summarized in the look-up tables, the authors realized that the NO
384 formed in the flame front region (Z_r = 1) even though it is not negligible, especially at high
385 temperature (i.e: like the non-EGR case), was not considered to affect the NO in spray axis, this
386 amount of pollutant could be transported into the flame core increasing the content of this
387 specie in the inner region of the diesel flame.

388 To consider this latter phenomenon in the simplest possible way, equilibrium
389 conditions were assumed throughout the whole flame front region even though this is not
390 completely true in reality. Therefore the amount of NO formed in the flame front will be equal
391 to NO_{eq} (already tabulated) for Y_{O2exc} = 0 (stoichiometric conditions, Z_r = 1) and for a given
392 adiabatic combustion temperature (T_{ad}). Consequently, this temperature, the only unknown,
393 was tabulated as a function of initial mixture's temperature (T_{ini}) and the initial oxygen mass
394 fraction (Y_{O2ini}) by considering constant P and H conditions. The results are plotted in Figure 5
395 which corresponds to the third tabulated table of the proposed methodology.

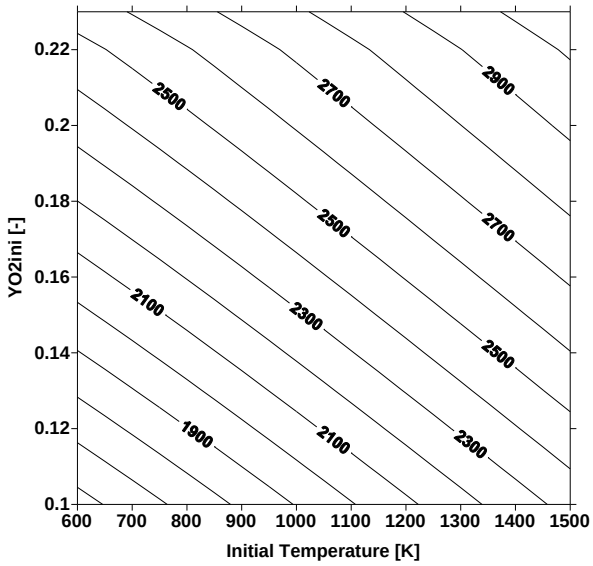

Figure 7.- Tabulated adiabatic combustion temperature as a function of initial mixture's temperature and initial oxygen mass fraction.

In Figure 8a and 8b the results yield considering this phenomenon are plotted. As expected, in both cases the over-prediction in the inner region of the flame is perfectly observed and diminishes rapidly as the flame front and the post combustion regions are reached ($Z_r \leq 1$). Finally the accuracy has increased significantly, specially in the massive EGR case (i.e.: 85% accuracy), suggesting that the methodology is accurate enough to perform not only qualitative but also quantitative predictions of NO formation in both scenarios.

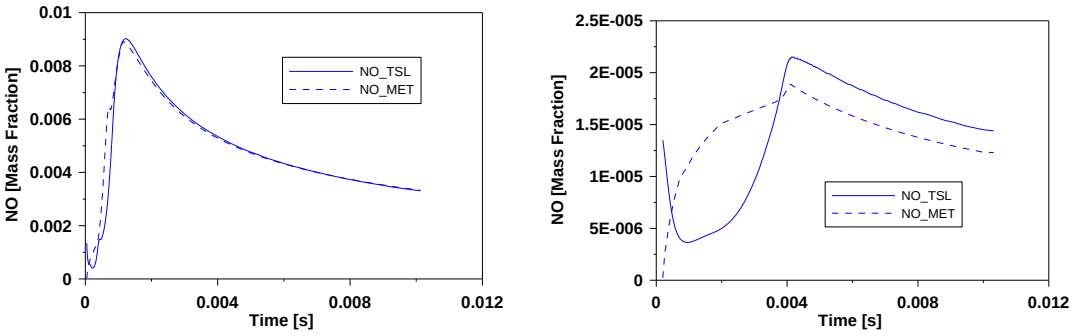

a) ***b)***

Figure 8.- Accuracy between the NO predicted by the proposed methodology (NO_MET) and by the TSL model considering the whole NO_x sub-mechanism included in GRI-Mech 3.0 (NO_TSL), in the inner region of a diesel diffusion flame, for: a) Y_{O2ini} = 0.23 and b) Y_{O2ini} = 0.1, with n-heptane at a pressure 10MPa.

412

413 4.2. Validation with real engine-out NO_x measurements

414 The proposed methodology was validated against real engine NO_x measurements by
415 including it in the apparent combustion time model (ACT model) [34] and by comparing its
416 predictions with the ones yield by the original version of the ACT model. In Table 3 the engine
417 and the injector's characteristics used for real engine measurements are summarized while in
418 Table 4 the upper and lower limits of the key combustion parameters modified for these real
419 engine experiments are presented. A total of 42 cases were considered.

Engine's Characteristics	**Values**
Stroke [m]	0.15
Bore [m]	0.12
Compression ratio [-]	14.26
Connecting rod length [m]	0.225
Injector	**Values**
Num. Orifices	8
Diam. Orifice [μm]	100
Included angle [º]	140

420

421 ***Table 3.- Summary of the engine's and the injector's geometric specifications used for the***
422 ***engine test validation.***

423

Parameters	Units	Lower limit	Upper limit
Inj. Press.	(bar)	1645	2350
SOI	(CAD)	-24	-12
Intake Press.	(bar)	1,49	3,555
Speed	(rpm)	1200	1200
Air mass	(kg/h)	59,33	89,56
Fuel mass	(mg/cc)	90,48	130,292
EGR	(%)	30,03	75,31
NOx	(ppm)	3,04	684,44
Fr	(-)	0,60	0,80
XO2 intake	(%)	8,67	15,99
YO2 intake	(%)	10,10	17,33

424

425 ***Table 4. Summary of the key combustion parameters modified for real engine testing.***

426 Initially, the predictions of the original ACT model in comparison with the engine
427 results, plotted in Figure 9a, show a considerable under-prediction of this pollutant in the LTC
428 region (low NO formation and combustion temperatures) while for the CDC conditions (high
429 NO formation and combustion temperatures) the accuracy is high. These results are in
430 accordance with the fact that this version only considers the thermal mechanism which is
431 directly dependent on temperature, the higher the temperatures the higher the relevancy.

432 In the case of including all the formation routes (ACT_MET), blue squares in Figure 9a,
433 the accuracy of the predictions in the low NO formation region is slightly improved while no
434 major changes occur at high NO formation region, just as expected.

435 Afterwards, the same engine results were compared with the new version of the ACT
436 model see Figure 9b. In this case the original version used to predict the chemical phenomena
437 related with the NO formation was replaced by the proposed methodology (all formation
438 routes and NO transport from flame front to flame core). As it can be observed from Figure 9b
439 the accuracy is substantially higher even in the low NO formation region. Therefore, it can be
440 concluded that the proposed methodology substantially improves the original version of the

ACT model and is sufficiently accurate to perform, at least, qualitative predictions for engine-out NO_x emissions without demanding high computational resources.

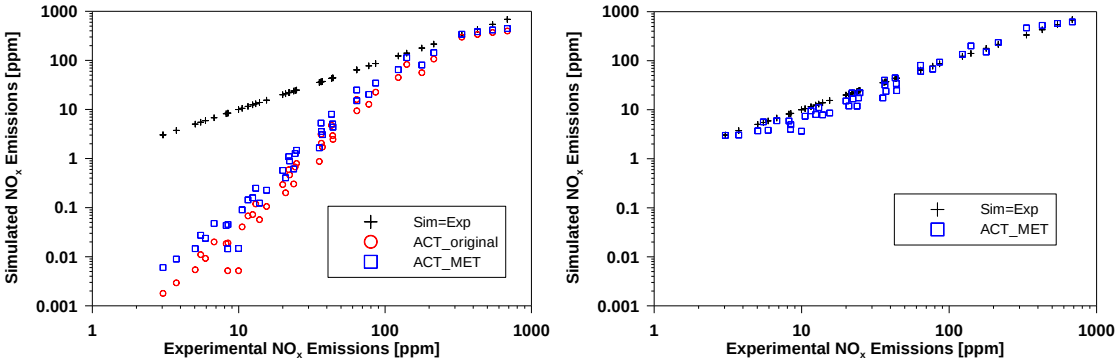

Figure 9.- Comparison between real engine NO emissions measurements (black crosses) and the prediction of: a) original ACT model and b) new ACT model.

5. Conclusions

After analyzing the results obtained, the conclusions that can be extracted from the present study are the following:

a. The NO_x sub-mechanism employed from the GRI-Mech 3.0 mechanism can be considered as a first order reversible reaction for the vast majority of the studied conditions. Only at very low temperatures (T < 1300K) and independently of the equivalence ratio, this simplification is little effective.

b. The k-values obtained are in accordance with the chemistry ruling the NO formation process. They reflect that the thermal mechanism is the predominant route at high temperatures, vertical iso-k lines, and as the temperature decreases so does its predominance in favor of the prompt and the N_2O routes. This causes the iso-k lines to slightly curve or get distorted.

c. The hypothesis in which the present methodology is based on was satisfactorily validated in the diffusion diesel combustion (e.g: diesel spray) scenario. The methodology reproduces, even when massive EGR is considered, the temporal evolution of NO with a reasonable accuracy. Consequently, the author believes that the 0-D low cost methodology proposed in the present paper has enough favorable arguments to be considered for future simulations.

d. The accuracy of the predictions is reasonably high if compared with real engine measurements when considering the transport effect of NO from the flame front region into the flame core. This fact corroborates that the present methodology can be used to predict NO_x emissions in real engines.

Acknowledgements:

The authors would like to acknowledge the contribution of the Spanish Ministry of Economic and Competitively for the financial support of the present research study associate to the projects TRA 2008-06448 (VELOSOOT).

References:

[1] Desantes J. M., López J. J., Redon P., Arrégle J. "Evaluation of the thermal NO formation mechanism under low-temperature diesel combustion conditions" International Journal of Engine Research 13 (6) 531-539. 2012.

[2] Musculus M. "Multiple simultaneous optical diagnostic imaging of early-injection low-temperature combustion in a heavy-duty diesel engine". SAE Paper: 2006-01-0079. 2006.

[3] Zeldovich Y.B. "The oxidation of nitrogen in combustion and explosion". Acta Physicochim 1946; 21: 577-628.

[4] Glarborg P., Miller J.A. "Mechanism and Modeling of Hydrogen-Cyanide Oxidation in a Flow Reactor". Combustion and Flame 99, Issue 3-4, pp: 475-483, 1994.

[5] Miller J.A., Bowman C.T. “Mechanism and modeling of nitrogen chemistry in combustion”. Progress in Energy and Combustion Science, Volume 15, pp: 287-338, 1989.

[6] Dean A.M., Bozelli J. W. Gas-Phase Combustion. Nitrogen Combustion Chemistry (pp:124-343). Editor W. C. Gardiner Jr. 1999

[7] Amnéus P., Mauss F., Kraft M., Vressner A., Johansson B. "NO_x and N_2O formation in HCCI Engines". SAE Paper no: 2005-01-0126. 2005.

[8] Kung E.H., Mauss F., Priyadarshi S., Nese B.C., Haworth D.C. “A CFD investigation of emissions formation in HCCI engines, including detailed NO_x chemistry” Multidimensional Engine Modeling Users Group Meeting, 2006.

[9] Dec J.E. “A conceptual model of DI diesel combustion based on laser-sheet imaging.” SAE Trans 1997; 106: 1310-1348. SAE Paper no: 970873. 1997.

[10] Fenimore C.P., editors. "Formation of Nitric Oxide in Premixed Hydrocarbon Flames". Proceedings of the 13th International Symposium on Combustion; 1971. Pittsburgh, USA.

[11] Miller J.A., Branch M.C., McLean W.J, Chandler D.W., Smooke M.D., Kee R.J. “The conversion of HCN to NO and N_2 in H_2-O_2-HCN-Ar Flames at Low Pressure”. Symposium (International) on Combustion, Volume 20, pp: 673-684, 1985.

[12] Smooke M.D., Mitchell R.E., Keyes D.E. “Reduced Kinetic Mechanisms and Assymptotic Approximations for Methane-Air Flames”. Combustion Science Technology 67:85. 1989.

[13] Keck J.C., Gillespie D. “Rate-controlled Partial Equilibrium Method for Treating Reacting Gas Mixtures”. Combustion and Flame. Volume 17. pp: 237-241. 1971.

[14] Chen J.Y., Dibble R.W. “Application of Reduced Mechanisms for Prediction of Turbulent Nonpremixed Methane Jet Flames” in Lecture Notes in Physics 384 “Reduced Kinetic Mechanisms and Asymptotic Approximations for Methane-Air Flames”. Edited by M. D. Smooke, Ed.), pp: 193-226, 1991..

[15] Peters N., Kee R.J. “The Computation of Stretched Laminar Methane-Air Diffusion Flames using a Reduced Four-Step Mechanism” Combustion and Flame 68, 1, 17-29, 1987.

[16] Chen J-Y. “A General Procedure for Constructing Reduced Reaction Mechanisms with given Independent Relations”. Combustion Science Technology. 57, 1-3, 89-94. 1988.

[17] Lam S.H., Goussis D.A. “Conventional Assymptotic and Computational Singular Perturbation for Simplified Kinetics Modeling”. Technical Report #1864(a)-MAE, Princeton University, 1991.

[18] Pope S.B. “Computationally efficient implementation of combustion chemistry using in situ adaptive tabulation” Combustion Theory Modelling (1), pp: 41-63, 1997.

524 [19] Maas U., Pope S.B. “Simplifying chemical kinetics: Intrinsic low-dimensional manifolds in
525 composition space” Combustion and Flame, Volume 88, Issue 3-4, pp: 239-264, 1992.
526 [20] Gicquel O., Darabiha N., Thévenin D. “Laminar premixed hydrogen/air counterflow flame
527 simulations using flame prolongation of ILDM with differential diffusion.” Proceedings
528 of the Combustion Institute, Volume 28, pp: 1901-1908, 2000.
529 [21] Pera C., Colin O., Jay S. “Development of a FPI detailed chemistry tabulation methodology
530 for internal combustion engines.” Oil & Gas Science and Technology-rev. IFD, 64, 243-
531 258, 2009.
532 [22] Van Oijen J., de Goey L. “Modelling of Premixed Laminar Flames using Flamelet-
533 Generated Manifolds.” Combustion Science Technology, Volume 161, pp: 113-137,
534 2000.
535 [23] Ribert G., Gicquel O., Darabiha N., Veynante D. “Tabulation of complex chemistry based
536 on self-similar behavior of laminar premixed flames.” Combustion and Flame, Volume
537 146, pp: 649-664, 2006.
538 [24] Fusco A., Knox-Kelecy A.L., Foster D.E. “Application of phenomenological soot model to
539 diesel engine combustion” International symposium Comodia 94, 1994.
540 [25] Merker G.P., Hohlbaum B., Rauscher M. "Two-zone model for calculation of Nitrogen-
541 oxide formation in Direct-Injection Diesel Engines". SAE Paper no: 932454. 1993.
542 [26] Rakopoulos C.D., Antonopoulos K.A., Rakopoulos D.C. “Development and application of
543 multi-zone model for combustion and pollutants formation in direct injection diesel
544 engine running with vegetable oil or its biodiesel”. Energy Conversion and
545 Management Volume 48, pp: 1881-1901, 2007.
546 [27] Zheng J., Caton J.A. “Use of a Single-Zone Thermodynamic Model with Detailed Chemistry
547 to Study a Natural Gas Fueled Homogeneous Charge Compression Ignition Engine”.
548 Energy Conversion and Management. Volume 53, Issue 1, pp: 298-304, 2012.
549 [28] Easley W.L., Mellor A.M., Plee S.L. "NO formation and Decomposition models for DI
550 Diesel Engines". SAE Paper no: 2000-01-0582. 2000.
551 [29] Elkelawy M., Zhang Y.S., El-Din H.A., Yu J.Z. Society of Automotive Engineers. SAE paper
552 no: 2008-01-1706. 2008.
553 [30] Ng C.K., Thomson M.J.A. “Computational Study of the Effect of Fuel Reforming, EGR and
554 Initial Temperature on Lean Ethanol HCCI Combustion”. SAE paper no: 2004-01-0556.
555 2004.
556 [31] Gupta H., Mallikarjuna, J.M. “Thermo-Kinetic Model to Predict Start of Combustion in
557 Homogeneous Charge Compression Ignition Engine” International Conference on

558 Mechanical, Production and Automobile Engineering (ICMPAE'2011) Pattaya Dec.
559 2011.
560 [32] Kee R.J., Rupley F.M., Miller J.A., Coltrin M.E., Grcar J.F., Meeks E., et al., "CHEMKIN
561 Release 4.0". Reaction Design, Inc., San Diego, CA; 2004.
562 [33] Broadwell J. E., Lutz A. E. “A Turbulent Jet Chemical Reaction Model: NO_x Production in
563 Jet Flames” Combustion and Flame, Volume 114, pp: 319-335, 1998.
564 [34] Arrègle J., Lopez J.J., Martin J., Mocholí E. “Development of a Mixing and Combustion
565 Zero-Dimensional Model for Diesel Engines”. SAE Paper no: 2006-01-1382. 2006.
566 [35] Seiser H., Pitsch H., Seshadri K., Pitz W.J., Curran H.J., "Extinction and Autoignition of n-
567 Heptane in Counterflow Configuration", Proceedings of the Combustion Institute,
568 Volume 28, pp: 2029-2037, 2000.
569 [36] Gregory P. Smith, David M. Golden, Michael Frenklach, Nigel W. Moriarty, Boris Eiteneer,
570 Mikhail Goldenberg, C. Thomas Bowman, Ronald K. Hanson, Soonho Song, William C.
571 Gardiner, Jr., Vitali V. Lissianski, and Zhiwei Q.
572 in http://www.me.berkeley.edu/gri_mech/.
573 [37] Farrell J.T., Cernansky N.P., Dryer F.L., Friend D.G., Hergart C.A., Law C.K., et. al.
574 "Development of an Experimental Database and Kinetic Models for Surrogate Diesel
575 Fuels". SAE Paper no: 2007-01-0201. 2007.
576 [38] Asif Faiz, Christopher S. Weaver, Michael P. Walsh., “Air pollution from motor vehicles.
577 Standards and technologies for controlling emissions.” Ed. The International Bank.
578 1996. ISBN:0-8213-3444-1.
579 [39] Han, M. “The effects of synthetically designed diesel fuel properties-cetane number,
580 aromatic content, distillation temperature, on low combustion temperature”. Fuel
581 109, pp: 512-519, 2013.
582 [40] Benajes J., Lopez J.J., Novella R., Redon P. “Comprehensive modeling study analyzing
583 the insights of the NO-NO_2 conversion process in current diesel engines”.
584 Energy Conversion and Management, Volume 84, pp: 691-700, 2014.
585 [41] Peters N. "Turbulent Combustion". United Kingdom: Cambridge University Press United
586 Kingdom; 2000.
587 [42] Payri F., Arrègle J., López J.J. and Mocholí E (2008) “Diesel NO_x Modeling with a Reduction
588 Mechanism for the Initial NO_x Coming from EGR or Re-entrained Burned Gases”. SAE
589 paper no: 2008-01-1188. 2008.
590 [43] Davis M.E., Davis R.J. “Fundamentals of Chemical Reaction Engineering” Editorial Mc.
591 Graw-Hill. New York. 2003.

592 [44] Heywood J.B. "Internal combustion engines fundamentals". Editorial Mc. GrawHill. New
593 York. 1988.
594 [45] Idicheria C.A., Pickett L.M. “Formaldehyde Visualization Near Lift-Off Location in a Diesel
595 Jet”. SAE Paper no: 2006-01-3434. 2006.
596 [46] Glarborg, P., Kee, R. J., Miller, J. A. “Kinetic Modeling and Sensitivity Analysis of Nitrogen
597 Oxide Formation in Well-Stirred Reactors”. Combustion and Flame 65:177 (1986).
598 [47] Meunier, P. H., Costa, M., Carvalho, M. G. “The Formation and Destruction of NO in
599 Turbulent Propane Diffusion Flames”. Fuel, Volume 77, No. 15, pp: 1705-1714, 1998.
600 [48] Dupont, V., Williams, A. “NOx Mechanisms in Rich Methane-Air Flames”. Combustion and
601 Flame, Volume 114, pp:103-118, 1998.
602
603
604
605
606

Appendix A: Mathematical demonstration of how the NO_x sub-mechanism behaves as a pseudo first order reversible reaction

In the present research study, the author has obtained an empirical fit equation (Eq.A1), which corresponds to a pseudo first order reversible reaction, to characterize the NO/NO_{eq} temporal evolution at constant pressure and temperature conditions and considering the whole NO_x sub-mechanism included in the GRI-Mech 3.0 chemical-kinetic mechanism. Consequently, this fact seems to suggest that the whole sub-mechanism can be treated as a pseudo first order reversible reaction.

$$\frac{NO}{NO_{eq}} = \left(1 - e^{-k \cdot t}\right) \quad \textbf{(Eq. A1)}$$

To confirm such finding, the author will try to demonstrate that the fit equation can be achieved by applying the chemical-kinetic science.

Initially, the type of reactions considered in the NO_x sub-mechanism can be written, in a general manner, as:

$$aA + bB = cC + dD \quad \textbf{(Eq.A2)}$$

and characterized by k_f and k_b which correspond to the forward and backward reaction constants, respectively. Note that A, B, C and D each stand for a chemical specie and a, b, c and d are the corresponding coefficients. The equal sign symbolizes that the reaction is reversible, which means, it can occur forward (yielding the species C and D) or backwards (yielding the species A and B).

The reaction rate law, for a pseudo first order reversible reaction, can be expressed by Eq. A3 and the variation in concentration for reactant A and product C can be described as Eq. A4 and Eq. A5, respectively.

$$\frac{dC}{dt} = k_f[A] - k_b[C] \quad \textbf{(Eq.A3)}$$

$$[A] = [A_o] - ax \quad \textbf{(Eq.A4)}$$

$$[C] = [C_o] + cx \quad \textbf{(Eq. A5)}$$

Where $[A_o]$, $[C_o]$, [A] and [C] are the initial and final moles of the chemical specie A and C, respectively and x is a latent variable which describes the conversion degree.

Substituting Eq. A4 and A5 into Eq. A3 will yield the following expression (Eq. A8):

$$\frac{dC}{dt} = C * \frac{dx}{dt} \quad \textbf{(Eq. A6)}$$

$$K_c = \frac{k_f}{k_b} \quad \textbf{(Eq. A7)}$$

$$\frac{dx}{dt} = \frac{1}{C}\left(k_f([A_o] - ax]) - \frac{k_f}{K_c}([C_o] + cx)\right) \quad \textbf{(Eq. A8)}$$

Simplifying this latter equation by defining a new constant (Eq. A9) and rearranging it with basic algebra, the following expressions are yield:

$$\mathbf{cte} = \mathbf{A_o} - \frac{\mathbf{C_o}}{\mathbf{K_c}} \quad \textbf{(Eq. A9)}$$

$$\int_0^x \frac{\mathbf{C}\cdot\mathbf{dx}}{\left(\mathbf{cte} - \mathbf{ax} - \frac{\mathbf{cx}}{\mathbf{K_c}}\right)} = \int_0^t \mathbf{k_f}\cdot\mathbf{dt} \quad \textbf{(Eq. A10)}$$

$$\int_0^x \frac{\mathbf{C}\cdot\mathbf{dx}}{\left(\mathbf{cte} - \mathbf{x}\cdot\left(\mathbf{a} + \frac{\mathbf{c}}{\mathbf{K_c}}\right)\right)} = \int_0^t \mathbf{k_f}\cdot\mathbf{dt} \quad \textbf{(Eq. A11)}$$

Renaming what is inside the brackets, multiplying the x variable, with Eq. A11 and solving the integral in both sides will result in Equation A13.

$$\mathbf{cte_2} = \mathbf{a} + \frac{\mathbf{c}}{\mathbf{K_c}} \quad \textbf{(Eq. A12)}$$

$$-\frac{\mathbf{C}}{\mathbf{cte_2}}\cdot\left[\ln(\mathbf{cte} - \mathbf{cte_2}\cdot\mathbf{x}) - \ln(\mathbf{cte} - \mathbf{0})\right] = \mathbf{k_f}\cdot\mathbf{t} \quad \textbf{(Eq. A13)}$$

Re-arranging with basic algebra:

$$\mathbf{x} = \frac{\mathbf{cte}\cdot\left(\mathbf{1} - \mathbf{e}^{-\mathbf{cte_2}\cdot\mathbf{k_f}\cdot\mathbf{t}}\right)}{\mathbf{cte_2}} \quad \textbf{(Eq. A14)}$$

To solve for the equilibrium conditions two procedures, which yield the same result, can be used indistinctively. The first of them is to calculate x_{eq}, with Equation A15, assuming that t tends to ∞ and the second is to apply the condition that at equilibrium $\frac{dx}{dt} = 0$ and proceed in a similar way as previously. In this case, to simplify the calculations, the first procedure will be employed.

$$\mathbf{x_{eq}} = \frac{\mathbf{cte} - \mathbf{0}}{\mathbf{cte_2}} = \frac{\mathbf{cte}}{\mathbf{cte_2}} \quad \textbf{(Eq. A15)}$$

Dividing x by x_{eq} and substituting x by NO and redefining the power coefficient, as described in Eq. A16, will result in Eq. A17.

$$k = cte_2 \cdot k_f \qquad \textbf{(Eq. A16)}$$

$$\frac{NO}{NO_{eq}} = \frac{cte \cdot (1 - e^{-k \cdot t})/cte_2}{(\frac{cte}{cte_2})} = \left(1 - e^{-k \cdot t}\right) \qquad \textbf{(Eq. A17)}$$

As it can be appreciated, Eq. A17 is identical to Eq. A1. This confirms that the whole NO_x sub-mechanism can be treated as a pseudo first order reversible reaction for the tested conditions.

Appendix B: Mathematical demonstration of how the equation in which the methodology is based on is yield from the fit equation

In the following appendix the mathematical demonstration of how equation (Eq. B0) is obtained from the fit equation (Eq. B00) is described.

$$NO_t = NO_{t-1} + k * (NO_{eq} - NO_{t-1}) * (t_t - t_{t-1}) \quad \textbf{(Eq. B0)}$$

$$\frac{NO}{NO_{eq}} = 1 - \exp(-k \cdot t) \quad \textbf{(Eq. B00)}$$

Equation B0 is reached by substituting the derivative terms of equation B1 by differences, resulting in equation B2. If these differences are between two consecutive points, denoted as t and t-1, then equation B3 is obtained. This equation is the same as equation B0.

$$\frac{dNO}{dt} = k \cdot (NO_{eq} - NO) \quad \textbf{(Eq. B1)}$$

$$\Delta NO = k \cdot (NOeq - NO) \cdot \Delta t \quad \textbf{(Eq. B2)}$$

$$NO_t - NO_{(t-1)} = k * (NO_{eq} - NO_{t-1}) \cdot (t - t_{t-1}) \quad \textbf{(Eq. B3)}$$

Regarding equation B00, the starting point is also equation B1. Rearranging it with basic algebra and integrating it throughout the boundary conditions used in the characterization process will yield equation B4.

$$\frac{dNO}{dt} = k \cdot (NO_{eq} - NO) \quad \textbf{(Eq. B1)}$$

$$\int_0^{NO} \frac{dNO}{(NO_{eq} - NO)} = k * \int_0^t dt \quad \textbf{(Eq. B4)}$$

If the resulting equation of this integration procedure, (Eq. B5), is rearranged mathematically and multiplied both sides by the inverse of natural logarithm, the equation B6 will be obtained.

$$-[\ln(NO_{eq} - NO) - \ln(NO_{eq} - 0)] = k \cdot (t - 0) \quad \textbf{(Eq. B5)}$$

$$\frac{NO_{eq} - NO}{NO_{eq}} = \exp(-k \cdot t) \quad \textbf{(Eq. B6)}$$

Finally, further algebraically rearrangements will yield equation B7 which is identical to the fit equation (Eq. B00).

$$\frac{NO}{NO_{eq}} = 1 - \exp(-k \cdot t) \quad \textbf{(Eq. B7)}$$